Modeling of the power-dependent velocity of microwave magnetic envelope solitons in thin films

C. E. Zaspel[a)]
Department of Physics, Montana State University, Bozeman, Montana 59717

P. Kabos, H. Xia, H. Y. Zhang, and C. E. Patton
Department of Physics, Colorado State University, Fort Collins, Colorado 80523

(Received 5 October 1998; accepted for publication 5 March 1999)

Recently obtained single soliton solutions to the nonlinear Schrödinger equation with additional higher order nonlinear and dispersion terms have been used to model the properties of microwave magnetic envelope solitons in thin films and, in particular, the recently observed power-dependent soliton velocity in these films. The modeling is based on an empirical scaling between the dimensionless amplitude parameters in the higher order nonlinear Schrödinger (HONLS) equation and the pulse power levels in the experiment. Based on this scaling, the amplitude-dependent soliton velocity from the HONLS equation solution is shown to match the velocity versus power response from the experiment. © *1999 American Institute of Physics.* [S0021-8979(99)01112-3]

I. INTRODUCTION

It is now well established that yttrium iron garnet (YIG) films can support microwave magnetic envelope (MME) solitons. These structures are produced in magnetized thin films at a microstrip antenna fastened to the film. An amplitude modulated microwave frequency input pulse is launched at the input antenna and it is detected at a second antenna a few millimeters from the first. As the pulse propagates between the two antennas it evolves into a soliton, which is a nonlinear pulse that propagates with no change in shape. Such soliton excitations have been generated, propagated, and collided in YIG films for various external field orientations and surface pinning conditions.[1–6] The nonlinear Schrödinger (NLS) equation[7,8] has been used to model the decay properties[6] and both pulse profiles and the power response[9] with good accuracy.

However, one critical problem between theory and experiment remains. This concerns the recently observed power-dependent MME soliton velocity.[10] The data show a small but significant increase in the soliton velocity from the usual low power magnetostatic wave (MSW) group velocity with increasing power. In contrast, the hyperbolic secant order one soliton solution to the NLS equation has an arbitrary but amplitude-independent velocity. For the pulse shape and power response modeling in Ref. 9, this velocity was set at the MSW group velocity. Although there appears to be some connection between velocity plateaus as a function of power and modulational instability processes,[10] there has been no real physical explanation of the observed power response in the soliton velocity.

This article describes recent work to improve the modeling of this velocity response for MME solitons. The improvement has been achieved through the use of a higher order nonlinear Schrödinger (HONLS) equation which contains third order and nonlinear dispersion terms, and through the exact order one soliton solutions to this equation reported by Gedalin *et al.*[11] A remarkable feature of this new solution is a dependence of the HONLS solitary wave velocity on the solitary wave amplitude. This new solution, moreover, appears to model the MME soliton velocity data from Ref. 10 quite well.

II. THE HONLS EQUATION

The HONLS equation in Ref. 11 for an wave packet envelope response function $\phi(z,t)$ may be written in the form

$$i\phi_t + \frac{D_2}{2}\phi_{zz} - N|\phi|^2\phi - i\left[\frac{D_3}{6}\phi_{zzz} - Q(|\phi|^2\phi)_z\right] = 0. \tag{1}$$

The ϕ parameter denotes the amplitude of the $\phi(z,t)$ response function at a given position z and time t, where the z coordinate is measured in a reference frame which moves with the usual low power limit group velocity v_g. In the context of MME solitons, the complex $\phi(z,t)$ response function is usually taken to represent the dynamic magnetization response normalized to the static saturation magnetization M. For the present purposes, the convention of Ref. 3, will be adopted.

The t and z subscripts in Eq. (1) denote partial differentiation with respect to time and position, respectively. The $i\phi_t$, $D_2\phi_{zz}/2$, and $N|\phi|^2\phi$ terms constitute the usual nonlinear Schrödinger equation, with D_2 as the linear dispersion parameter and N as the nonlinear frequency response parameter. The higher order terms are contained in the square bracket expression on the left side of Eq. (1). The D_3 parameter is a third order linear dispersion coefficient and Q denotes a nonlinear dispersion parameter.

The various terms in Eq. (1) can be obtained from the method of envelopes[12] and the nonlinear spin wave dispersion relation. The coefficients of the various terms, so obtained, are

a)Electronic mail: zaspel@physics.montana.edu

 © 1999 American Institute of Physics

$$D_n=\frac{\partial^n \omega_k}{\partial k^n}, \tag{2}$$

$$N=\frac{\partial \omega_k}{\partial |\phi|^2}, \tag{3}$$

and

$$Q=\frac{\partial N}{\partial k}. \tag{4}$$

The spin wave frequency ω_k is taken to be a function of both the spin wave number k and the amplitude ϕ according to $\omega=\omega(k,|\phi|^2)$. In order to obtain the operational parameters for Eq. (1), the derivatives in Eqs. (2) through (4) are evaluated at the operating point wave number k_0 and frequency ω_0 of interest, and at $|\phi|^2=0$. These evaluations depend on the specific nature of the magnetic excitation under consideration.

The above equations yield a solitary wave single pulse solution given by[11]

$$\phi(z,t)=\phi_0 \cosh^{-1}[\alpha\phi_0(z-v_s t)]e^{i(\kappa z-\Omega t)}, \tag{5}$$

where ϕ_0 is the pulse amplitude. The other as yet undefined parameters in Eq. (5) are given by

$$\alpha=\sqrt{-\frac{3Q}{D_3}}, \tag{6}$$

$$\kappa=\frac{N}{2Q}-\frac{3D_2}{2D_3}, \tag{7}$$

$$v_s=D_2\kappa\left(1+\frac{D_3\kappa}{2D_2}\right)+\frac{Q}{2}\phi_0^2, \tag{8}$$

and

$$\Omega=\frac{\kappa^2}{2}\left(D_2+\frac{D_3\kappa}{3}\right)+\frac{QD_3}{12D_2^2}\left(1+\frac{D_3\kappa}{D_2}\right)\phi_0^2. \tag{9}$$

Note that $\phi(z,t)$ represents the complex envelope function for the MME wave packet and contains no carrier response. This means that the κ and Ω parameters in the complex exponential of Eq. (5) correspond to wave number and frequency deviations from the operating point carrier wave number k_0 and carrier frequency ω_0, respectively. Note also that only the shape of the complex envelope, $\phi(z,t)$, the amplitude ϕ_0, and the solitary wave velocity v_s are accessible in conventional MME pulse experiments.

The important theoretical result for the present purposes is the velocity expression of Eq. (8) and, in particular, the dependence of the soliton velocity on ϕ_0^2. Since ϕ_0^2 scales with power, Eq. (8) predicts a power-dependent soliton velocity. It is this result which makes possible a direct connection with the recent experimental discovery of a power-dependent MME soliton velocity.[10] Keep in mind that Eq. (8) gives the solitary wave velocity in a reference frame which is moving at the low power limit group velocity v_g, so that the velocity given in Eq. (8) represents the additional velocity of the wave packet imposed by the HONLS equation. As will be shown shortly, the predicted ϕ_0^2 velocity response in Eq. (8) matches the experimental results quite well.

It is important to note that the HONLS equation is much more complicated than the NLS equation and that the solution of Eq. (5) does not go over to the hyperbolic secant single soliton solution to the NLS equation in the limit $Q\rightarrow 0$ and $D_3\rightarrow 0$. Moreover, the well-known Lighthill criteria for solitons which applies to the NLS equation, $N\cdot D_2<0$, does not appear explicitly in the HONLS analysis. As a precursor to further work with the HONLS equation as a possible model for real solitons, it will be important for these issues to be addressed.

III. MME SOLITON DATA

The basic MME soliton experiment has been described previously [3–6] and the details will not be repeated here. The data presented below are on (a) peak output power versus peak input power for MME pulses over a range of powers from well below the single soliton threshold to somewhat above that threshold, and (b) MME pulse velocity versus input peak power over the same range. These particular data were obtained for a 15.7 μm thick YIG film. Peak input power levels up to about 1 W, as measured at the input transducer port, were possible.

The data were obtained with the YIG film strip oriented in the external magnetic field such that the magnetization was parallel to the film plane, and the pulse propagation direction was parallel to the field. For the case of unpinned surface spins, this is referred to as the magnetostatic backward volume wave (MSBVW) configuration. In this particular experiment, an external static magnetic field of 1150 Oe, a carrier frequency of 5 GHz, and 13 ns wide input pulses were used. The MSBVW operating point wave number for the above setup was about 200 rad/cm. The pulse velocity was obtained for pulses propagated over a distance of 6 mm between input and output microstrip antennas in a standard MSBVW transducer structure.

Under the above conditions, the nominal propagation time for the MME pulse from input to output was about 100 ns. This propagation time was comparable to the nominal relaxation time for the 5 GHz excitations in the YIG. It will be important to take this decay into account in comparing the HONLS prediction with experiment.

Figure 1 shows soliton output power versus input power characteristics. The solid circles in Fig. 1 show typical data for the output peak power as a function of the input peak power. These data show that the response is linear up to a nominal peak input power of about 0.2 W. For higher powers, the response is nonlinear. The three anomalous points for input powers above one watt or so are related to the onset of higher order soliton effects. The solid line shows a polynomial fit to the data with these points excluded.

While there is no clear break in the data to show an abrupt nonlinear onset, the change from the linear to a nonlinear response due to the beginning of the soliton formation process is clearly evident.[6] The power threshold for the beginning of this process will be set at 0.2 W, as indicated by the vertical down pointing arrow labeled P_{th} in Fig. 1.

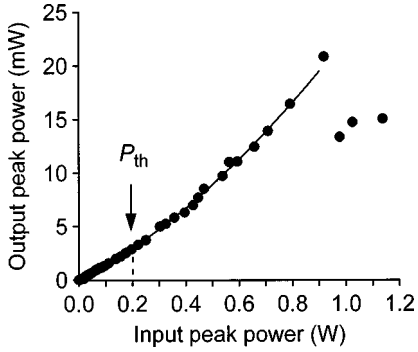

FIG. 1. Output peak power vs input peak power for MSBVW pulse propagation in a 15.7 μm thick yttrium iron garnet film. The in-plane static magnetic field parallel to the propagation direction was 1150 Oe, the microwave carrier frequency was 5 GHz, the input pulse width was 13 ns, and the transducer separation was 6 mm. The solid circles show the data. The solid line shows a polynomial fit to the data, with the three anomalous high power points excluded. The arrow labeled P_{th} denotes the approximate threshold input peak power for the beginning of soliton formation.

Figure 2 shows MSBVW soliton velocity versus power response characteristics. The solid circles show the velocity data for the experimental conditions given above. The solid crosses show results from the HONLS analysis to be discussed in the next section. The solid and dashed lines show polynomial fits to the HONLS analysis cross points and the solid circle data, respectively. These lines are intended to serve as a guide to the eye only. The nominal input power threshold point at $P_{th}=0.2$ W from Fig. 1 is also indicated.

The data in Fig. 2 show the basic experimental effect which is the subject of this work, a soliton velocity which increases with input power. For the experiment at hand, the velocity at low power, to be denoted as v_{th}, is about 6.47 cm/μs. It is important to note that the power response does not constitute a large effect. The data show a change in velocity over the available range of powers of about 3%–4%, similar to the results in Ref. 10.

IV. HONLS EQUATION VELOCITY ANALYSIS

The HONLS equation and the analytical single soliton solution were used to obtain the solid cross results in Fig. 2. The HONLS analysis is based on two assumptions related to the solitary wave amplitude parameter ϕ_0 and the peak powers from the soliton measurements. First, it is assumed that the square of the solitary pulse amplitude in the HONLS solution, ϕ_0^2, for any real microwave pulse detected at the output transducer in the experiment scales linearly with the measured output peak power P_{out}. This linear connection may be written as

$$\phi_{out}^2 = AP_{out}, \tag{10}$$

where ϕ_{out} is the value of ϕ_0 for the solitary wave pulse at the output antenna and A is a calibration factor.

Note that the value of ϕ_0 right after launch at the input antenna will typically be much larger than ϕ_{out}. Depending on the applicable decay rate for the nonlinear pulse, the initial value of ϕ_0 just after the soliton is formed may be greater than ϕ_{out} by a factor of $e^{+\eta_0 t_0}$ to $e^{+2\eta_0 t_0}$, where η_0 is the relaxation rate for the propagating MSBVW signals in the film and t_0 is the propagation time. The $e^{+\eta_0 t_0}$ factor applies to linear signals and the $e^{+2\eta_0 t_0}$ applies to solitons. Both factors are based on a soliton which is formed instantly at the input antenna. In actuality, the steepening and narrowing which leads to the soliton formation occurs over an appreciable portion of the propagation time, depending on the input power. These considerations are discussed in detail in Refs. 5 and 6.

For simplicity, the analysis below will use the $e^{+2\eta_0 t_0}$ soliton factor. For the experiments here, low power measurements yielded a decay rate η_0 of 9.6×10^6 rad/s. The 6 mm propagation distance and the measured velocity of 6.5×10^6 cm/s give an $\eta_0 t_0$ product of 0.89 which is close to unity. This means than ϕ_0^2 can vary by as much as e^4 from input to output. It will be necessary to take this variation into account in the evaluation of the HONLS velocity for comparison with experiment.

The coupling parameter A in Eq. (10) depends on many factors, including the antenna design, the MSBVW carrier properties, impedance considerations, etc. Note, however, that $|\phi(z,t)|$ corresponds to the normalized dynamic magnetization $|\vec{m}(z,t)|/\sqrt{2}M$. From the extensive MME soliton work cited above, it is known that the peak value of $|\vec{m}(z,t)|$ for solitons ranges from about 1% to 10% of M, so that ϕ_0 is in the range 10^{-2}–10^{-1}. This will be an important consideration in the fits to experiment.

For the second assumption, in the spirit of the data in Fig. 1, one takes the connection between the input peak power P_{in} and the output peak power P_{out} to be nonlinear for input power levels above P_{th}. For the present purposes, the P_{out} vs P_{th} connection will be expressed as

$$P_{out} = C(P_{in})P_{in}. \tag{11}$$

The response function $C(P_{in})$ is readily accessible from the experiment. This function may be obtained on a numerical, point-by-point basis, for example, directly from the data in Fig. 1. These considerations, in combination with the P_{th} threshold power point identified in Fig. 1 and the below threshold velocity v_{th}, are all that is needed to generate theoretical velocity versus input power curves from the HONLS analysis for comparison with experiment.

Turn now to the soliton velocity data and the HONLS response from Eq. (8). Keep in mind that Eq. (8) is for the

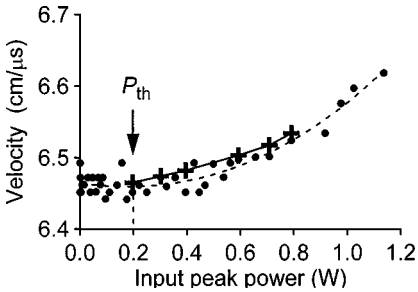

FIG. 2. Velocity as a function of input peak power for the MSBVW pulse propagation experiments. The solid circles show the data. The solid crosses show the HONLS results. The dashed and solid lines show polynomial fits to the data and the HONLS results, respectively. The arrow labeled P_{th} denotes the approximate threshold input peak power for the beginning of soliton formation.

solitary wave velocity in a frame of reference which is moving at the group velocity. The power dependence of this velocity is related only to the $\frac{1}{2}Q\phi_0^2$ term. The first term on the right hand side of Eq. (8) is independent of ϕ_0^2 and contributes only to a possible shift in the low power limit velocity of the pulse from v_g to $v_{\rm th}$. Furthermore, and as discussed above, the amplitude ϕ_0 is decreasing as the pulse propagates from input to output with an exponential decay rate which is somewhere between the linear decay rate η_0 and the soliton decay rate $2\eta_0$. For purposes of analysis, the soliton decay rate will be assumed. In this context, Eq. (8) may be integrated and combined with Eqs. (10) and (11) to obtain a theoretical expression for the power dependent average soliton velocity in the laboratory reference frame, $v_s^{(L)}$. The result may be written as

$$v_s^{(L)}=v_{\rm th}+A\frac{Q}{2}C(P_{\rm th})P_{\rm th}\left(\frac{C(P_{\rm in})P_{\rm in}}{C(P_{\rm th})P_{\rm th}}\right)F(\eta_0 t_0). \tag{12}$$

$$F(\eta_0 t_0)=\frac{1}{4\eta_0 t_0}(e^{4\eta_0 t_0}-1). \tag{13}$$

The $F(\eta_0 t_0)$ factor in the second term of Eq. (12) takes decay into account. In the decay free $\eta_0=0$ limit, the F factor reduces to unity. In a typical MME soliton experiment and as noted above, the condition $\eta_0 t_0\approx 1$ is more the case. That is, the propagation time and the decay time are about the same, and in the 100 ns range. This $\eta_0 t_0\approx 1$ approximation yields an F value of 13.6. This factor will be an important consideration in fitting Eq. (12) to the data of Fig. 2.

Apart from the F factor, the power-dependent term in Eq. (12) contains three parameters, A, Q, and $P_{\rm th}$, along with the empirical response function $C(P_{\rm in})$, the threshold value $C(P_{\rm th})$, and the input power variable $P_{\rm in}$. The nonlinear Q parameter may be evaluated from nonlinear MSBVW theory as outlined below. The $P_{\rm th}$ threshold and the $C(P_{\rm in})$ response function derive from the experimental power response data. Equation (12), therefore, provides a direct connection between the velocity data and the HONLS theory, with a single adjustable parameter A. As noted above, acceptable values of A, moreover, must be consistent with established limits on ϕ_0^2, which is expected to be in the range 10^{-4}–10^{-2}.

Recall that the Q parameter is simply the derivative of the nonlinear frequency response parameter N with respect to the wave number k. The Q parameter may be readily evaluated from the k-dependent nonlinear response function $N(k)$. Following the analysis of Ref. 7, one may evaluate N for in-plane magnetized films in the $k=0$ limit by writing the ferromagnetic resonance frequency as $\omega_{\rm FMR}=\{H[H+4\pi M(1-|\phi|^2)]\}^{1/2}$ and taking N as the derivative of $\omega_{\rm FMR}$ with respect to $|\phi|^2$. In order to evaluate Q, however, one needs a k-dependent N function. Slavin and Rojdestvensky[13] have obtained such an $N(k)$ with the same basic form as the Ref. 7 result, but with the magnetization M replaced by $M[1-P(k)]$, where $P(k)$ is given by

$$P(k)=1-\frac{1}{kL}(1-e^{-kL}). \tag{14}$$

The L parameter in Eq. (14) denotes the film thickness. The resulting $N(k)$ is given by

$$N(k)=\frac{|\gamma|4\pi MH[1-P(k)]}{2\sqrt{H\{H+4\pi M[1-P(k)]\}}}, \tag{15}$$

where $|\gamma|\approx 1.76\times 10^7$ rad/Oe s is the absolute value of the gyromagnetic ratio, $4\pi M\approx 1750$ G is the saturation induction for YIG, H is external magnetic field, and L is the film thickness. The numerical evaluation of N and Q for the experimental parameters cited above yields values of -8.7×10^9 rad/s and 4.6×10^6 cm/s, respectively. These same values may be obtained from numerical analysis of the MSBVW dispersion with the saturation magnetization M replaced by $M(1-|\phi|^2)$.

V. VELOCITY FITS FROM THE HONLS EQUATION ANALYTICAL SOLUTION

The working equations and procedures given above yield a soliton velocity which depends on the input peak power as specified in Eq. (12) with a single fitting parameter, the calibration factor A which connects $P_{\rm out}$ with $\phi_{\rm out}$. The solid cross points in Fig. 2 show the predicted velocity versus power response based on Eq. (12) and an A value of 0.15 $\rm W^{-1}$. The fit is quite reasonable.

For values of the input peak power in Fig. 1 from 0.2 to 0.8 W, the corresponding $P_{\rm out}$ values range from about 3 to 17 mW. For $A=0.15\,\rm W^{-1}$, the corresponding $\phi_{\rm out}$ values range from about 2×10^{-2} to 5×10^{-2}. These $\phi_{\rm out}$ values are well within the range applicable to solitons. If these amplitudes are taken to be on the order of $1/e$ of the amplitudes at the input antenna, the corresponding range of input amplitudes is from about 5×10^{-2} to 13×10^{-2}. These ϕ_0 values are also within the range applicable to solitons. The value of the coupling parameter A needed to fit the HONLS result to experiment appears, therefore, to be reasonable.

It is important to keep in mind that the $F(\eta_0 t_0)$ decay factor and the use of a soliton decay rate of $2\eta_0$ is critical to the realization of the physically acceptable ϕ_0 values which accompany the fit results given above. If this factor is ignored, the calibration factor A needed to fit the data must be over an order of magnitude larger than obtained above and this translates into unacceptably large ϕ_0 values. If one retains the $F(\eta_0 t_0)$ factor but uses the linear delay rate η_0, then A is somewhat larger than given above and the implied ϕ_0 values are marginal at best.

The simple decay analysis used here, moreover, does not account for the soliton formation processes or the conversion between soliton and nonsoliton propagation characteristics during propagation. In view of these complications, the best one can say is that the HONLS analysis appears to be consistent with the observed power dependent soliton velocity.

Further support of the above results was obtained through a numerical analysis of MME pulse propagation based on the HONLS equation but with damping included. The procedure was the same as outlined in Ref. 9, except that bandpass filtering of the output pulse profiles was not used. This analysis yielded numerical data which correspond to the experimental results in Figs. 1 and 2. The numerical output versus input power response curves were in the form of $\phi_{\rm out}^2$ vs $\phi_{\rm in}^2$ profiles, where $\phi_{\rm in}^2$ is the square of the reduced am-

plitude of a 13 ns rectangular input pulse. With appropriate scaling, these profiles had the same shape as the profiles in Fig. 1. This scaling could then be used to compute velocity response curves for comparison with the data and the HONLS equation analytical results in Fig. 2. These numerical velocity results were very close to the results shown in Fig. 2.

ACKNOWLEDGMENTS

This work was supported in part by the U.S. Army Research Office, Grant Nos. DAAH04-95-1-0325 and DAAG55-98-1-0430, the National Science Foundation, Grant Nos. DMR-9310967 and DMR-9801649. The YIG film used for the measurements was provided by Dr. D. Adam, Northrop Grumman Research and Development Laboratory, Pittsburgh, Pennsylvania. Dr. Kabos is on leave from the Slovak Technical University, Bratislava, Slovakia.

[1] B. A. Kalinikos, N. G. Kovshikov, and A. N. Slavin, Sov. Phys. JETP **38**, 413 (1983).
[2] P. DeGasperis, R. Marcelli, and G. Miccoli, Phys. Rev. Lett. **59**, 481 (1987).
[3] M. Chen, M. A. Tsankov, J. M. Nash, and C. E. Patton, Phys. Rev. B **49**, 12 773 (1994).
[4] M. A. Tsankov, M. Chen, and C. E. Patton, J. Appl. Phys. **76**, 4274 (1994).
[5] N. G. Kovshikov, B. A. Kalinikos, C. E. Patton, E. S. Wright, and J. M. Nash, Phys. Rev. B **54**, 15210 (1996).
[6] H. Xia, P. Kabos, C. E. Patton, and H. E. Ensle, Phys. Rev. B **55**, 15018 (1997).
[7] V. E. Zakharov and A. B. Shabat, Sov. Phys. JETP **34**, 62 (1972).
[8] A. Hasegawa and F. Tappert, Appl. Phys. Lett. **23**, 142 (1973).
[9] H. Y. Zhang, P. Kabos, H. Xia, R. A. Staudinger, P. A. Kolodin, and C. E. Patton, J. Appl. Phys. (in press).
[10] H. Xia, P. Kabos, R. A. Staudinger, and C. E. Patton, Phys. Rev. B **58**, 2708 (1998).
[11] M. Gedalin, T. C. Scott, and Y. B. Band, Phys. Rev. Lett. **78**, 448 (1997).
[12] G. P. Agrawal, *Nonlinear Fiber Optics* (Academic, Boston, 1995).
[13] A. N. Slavin and I. V. Rojdestvensky, J. Appl. Phys. **73**, 7007 (1993).